


Enthalpy-Entropy Compensation Effect in Chemical Kinetics and Experimental Errors: A Numerical Simulation Approach

Joaquin F. Perez-Benito* and Mar Mulero-Raichs

Departamento de Ciencia de Materiales y Quimica Fisica, Seccion de Quimica Fisica,
Facultad de Quimica, Universidad de Barcelona, Marti i Franques, 1, 08028 Barcelona,
Spain

 *Supporting Information*

ABSTRACT: Many kinetic studies concerning homologous reaction series report the existence of an activation enthalpy-entropy linear correlation (compensation plot), its slope being the temperature at which all the members of the series have the same rate constant (isokinetic temperature). Unfortunately, it has been demonstrated by statistical methods that the experimental errors associated with the activation enthalpy and entropy are mutually interdependent. Therefore, the possibility that some of those correlations might be caused by accidental errors has been explored by numerical simulations. As a result of this study, a computer program has been developed to evaluate the probability that experimental errors might lead to a linear compensation plot parting from an initial randomly scattered set of activation parameters (*p*-test). Application of this program to kinetic data for 100 homologous reaction series extracted from bibliographic sources has allowed concluding that most of the reported compensation plots can hardly be explained by the accumulation of experimental errors, thus requiring the existence of a previously existing, physically meaningful correlation.

1. INTRODUCTION

A common practice in chemical kinetics that provides useful information on the reaction mechanism is to study a series of closely related processes, differing among them either in the nature of an inert substituent in one of the reactant molecules^{1,2} or in the solvent employed to perform the experiments.^{3,4} An intriguing result often found in this kind of kinetic studies is the observation of a linear correlation between the activation parameters [activation energy (E_a) and logarithm of the pre-exponential factor (A) or, alternatively, enthalpy (ΔH°_\ddagger) and entropy (ΔS°_\ddagger) of activation] corresponding to the members of the homologous series.⁵

The existence of such linear relationship would be important at a theoretical level because it can be easily demonstrated that it would imply that at a certain temperature (called isokinetic temperature) all the members of the reaction series have the same rate constant.⁶ Unfortunately, it has been shown by statistical methods that the experimental errors associated with the activation energy and to the logarithm of the pre-exponential factor are not mutually independent. In fact, they are linearly related, with a slope that depends on the mean experimental temperature.⁷⁻¹⁰ The same can be stated with respect to the errors associated with the enthalpy and entropy of activation. As a consequence, when the divergences between the activation parameters for a series of related reactions are small in comparison with their respective experimental errors, a linear relationship tends to appear both in the E_a vs. $\ln A$ and ΔH°_\ddagger vs. ΔS°_\ddagger planes.

Because of this, some authors have considered that the existence of the so-called enthalpy-entropy compensation effect is a mere artefact derived from the experimental errors.^{11,12} However, other authors have argued that in certain cases, when the errors are quite small in comparison with the divergences between the activation parameters for the different members

of the reaction series, the linear correlation must be considered as physically meaningful and caused by a mechanism other than the experimental errors committed in the determination of the activation parameters. Several theories have been proposed to explain the origin of this statistically meaningful compensation effect. A comprehensive review developing some of them has been published.¹³ More recently, other theoretical interpretations of this phenomenon have been reported, such as the models of selective energy transfer (SET)¹⁴ or multiexcitation entropy.¹⁵ Nevertheless, although many different interpretations of the kinetic compensation effect have been propounded, a generally accepted theory is still missing.

An interesting point in this context is the fact that this kind of linear relationship tends to appear not only in the field of chemical kinetics, but also in other disciplines working with different processes ruled by mathematical laws of the type:

$$y = y_{\infty} e^{-\frac{x}{T}} \quad (1)$$

where y_{∞} is the value of the magnitude y at $T = T_{\infty}$ and x has the units of an absolute temperature. In the experimental studies involving this kind of equations it is often found that there exists a correlation between the values of x and y_{∞} , so that when one of them increases the other increases too. For instance, in chemical thermodynamics it has been found an enthalpy-entropy compensation effect for the temperature dependence of the equilibrium constants corresponding to many homologous reaction series (isoequilibrium relationship).¹⁶ In addition, similar compensation effects have been reported for a wide range of phenomena including those such as heating-induced changes in food chemistry,¹⁷ protein folding/unfolding and ligand binding/unbinding in biochemistry,¹⁸ as well as polymer

relaxation,¹⁹ thermal electron emission from semiconductor traps²⁰ and electron conduction in chalcogenide glasses²¹ in physics. Precisely, this ubiquitous character of the compensation effect makes it important as an objective of research.

2. METHODS

Random-Number Generators. Several programs were written in BASIC language in order to simulate the effect of accidental errors on the isokinetic relationships. All of them shared two different generators of random numbers, both starting with the calculation of the square root of a series of non-integer numbers, one in the increasing ($J + n$) and the other in the decreasing ($L + n$) directions, where J took the integer values from 1 to a fixed maximum limit (N) and L decreased in the opposite direction, n being a non-integer number (to avoid the occurrence of perfect squares). The random values were taken from the different decimal digits of the corresponding square roots (either $\sqrt{J + n}$ or $\sqrt{L + n}$), and an aleatory positive or negative sign was ascribed depending on the nature of the first digit (even or odd). These ensembles of random numbers were used with two finalities: to obtain a set of scattered couples ($\Delta H_{\neq}^{\circ}, \Delta S_{\neq}^{\circ}$) with no enthalpy-entropy correlation, and to simulate the accidental errors associated with the experimental determination of the rate constants at different temperatures.

Calculations. The statistical method used to obtain the best fit to a linear relationship was that of least squares. The absolute errors associated to the intercept and slope were the corresponding standard deviations.²² The hardware used in all the numerical simulations was

either a Sony Vaio or a Toshiba personal computer, and the software employed for the calculations was the programming language BBC BASIC (version for Windows).

3. EFFECTS OF EXPERIMENTAL ERRORS

As reported in the bibliography,⁷⁻¹⁰ when the temperature-rate-constant data are fitted according to an Arrhenius plot, the experimental errors associated with the pre-exponential factor and the activation energy are mutually interdependent. This result has been qualitatively illustrated in Figure 1. It can be observed that, when the laboratory uncertainties lead to a linear plot (green line) with a slope more negative than that corresponding to the real reaction, the intercept associated with $1/T = 0$ is higher than the value that would be obtained in the absence of errors (blue line). On the contrary, when the experimental errors lead to a linear plot (red line) with a slope less negative than that corresponding to the real reaction, the intercept is lower than that to be obtained in the absence of errors. This means that a positive error in the activation energy is usually associated with a positive error in the pre-exponential factor, whereas a negative error in the activation energy is usually associated with a negative error in the pre-exponential factor. Moreover, big errors in the activation energy are associated with big errors in the pre-exponential factor, whereas small errors in the first parameter are associated with small errors in the second.

Given the relationships existing between the activation energy and enthalpy on the one hand, as well as between the pre-exponential factor and the activation entropy on the other, this result can be easily extrapolated from the E_a vs. $\ln A$ plane to the $\Delta H_{\ddagger}^{\circ}$ vs. $\Delta S_{\ddagger}^{\circ}$ one.

Hence, it is clear that the ubiquity of experimental errors in all laboratory measurements should be considered as (at least) one of the possible explanations of the compensation effect: an increase of the activation energy (or the activation enthalpy) is usually associated with an increase of the pre-exponential factor (or the activation entropy), the former causing a decay of the reaction rate and the latter an enhancement, whereas a decrease of the first parameter (positive effect on the reaction rate) is very often associated with a decrease of the second (negative effect on the reaction rate), thus leading to the appearance of a compensation effect.

4. NUMERICAL SIMULATIONS

Parameters Involved. Some magnitudes had to be introduced at the beginning in order to perform the calculations. The first parameters required were the mean value (T_m) and the difference between the maximum and minimum values (ΔT) of the experimental temperature. All the programs had in common the same set of 5 simulated kinetics experiments, corresponding to the temperatures $T_m - (1/2) \Delta T$, $T_m - (1/4) \Delta T$, T_m , $T_m + (1/4) \Delta T$ and $T_m + (1/2) \Delta T$.

In this part of the present research, it has been taken as an initial hypothesis that the real activation parameters corresponding to the different members of the reaction series present no correlation at all, parameter F measuring the dispersion factor of the enthalpy and entropy of activation with respect to the assumed mean values ($\Delta H_{\neq, m}^0$ and $\Delta S_{\neq, m}^0$), according to the equations:

$$\Delta X_{\neq}^o = \frac{100}{100 + FA_N} \Delta X_{\neq, m}^o \quad (2)$$

$$\Delta X_{\neq}^o = \left(1 + \frac{FA_N}{100}\right) \Delta X_{\neq, m}^o \quad (3)$$

where $X = H$ or S , and A_N is an aleatory number ($0 \leq A_N \leq 10$), so that when $F = 1$ the maximum relative deviation with respect to the mean activation parameters is ± 10.0 %. These equations have been used to obtain activation parameters either lower (eq 2) or higher (eq 3) than the mean values, respectively, and were applied in a parity manner, each being responsible for a half of the simulated activation parameters.

An additional parameter necessary to start the simulations was the experimental error coefficient (Q), involved in the following equations relating the experimental (k_{exp}) and theoretical (k_{th}) rate constants:

$$k_{\text{exp}} = \frac{100}{100 + QA_N} k_{\text{th}} \quad (4)$$

$$k_{\text{exp}} = \left(1 + \frac{QA_N}{100}\right) k_{\text{th}} \quad (5)$$

This parameter quantifies the maximum uncertainty allowed to the laboratory determination of the rate constants, so that when $Q = 1$ the maximum relative accidental error is ± 10.0 %. Again, eqs 4 and 5 were applied in a parity manner, each being responsible for a half of the simulated error-affected rate constants. The theoretical rate constants were obtained from the

Eyring equation, using the activation parameters given by eqs 2 and 3, whereas their experimental counterparts were either lower (eq 4) or higher (eq 5) than them.

The final parameter required was the number of members of the homologous reaction series (N).

Results: Effect of the Dispersion Factor. By performing the numerical simulations using different values of parameter F , the effect of the dispersion factor on the activation enthalpy-entropy linear plot can be visualized (Figure 2). The points shown in purple represent the scattering of the activation parameters for the different members of the homologous reaction series, assuming as an initial hypothesis the absence of any real correlation between them, whereas those shown in blue represent the linearization caused by the experimental errors. When $F = 0$ (identical activation parameters for all the members of the reaction family), the plot is linear and with the slope almost identical to the mean experimental temperature. An increase of parameter F results in a decrease of both the apparent isokinetic temperature and the correlation coefficient (Table 1).

The value of the dispersion factor has been systematically changed from zero to a certain maximum limit, obtaining the parameters associated with each enthalpy-entropy compensation straight line for a family of $N = 1000$ simulated homologous reactions and repeating the calculations at five different mean experimental temperatures in the range 100–500 K. The resulting error-driven compensation plots have been fitted to equations of the type:

$$\Delta H_{\neq}^{\circ} = \Delta H_{\neq,0}^{\circ} + T_{ik} \Delta S_{\neq}^{\circ} \quad (6)$$

where the intercept ($\Delta H_{\neq,0}^{\circ}$) can be interpreted as the activation enthalpy for a hypothetical member of the reaction family with zero activation entropy and the slope (T_{ik}) is the apparent isokinetic temperature.

At low temperatures the intercept absolute error decreases monotonously as the value of the intercept corresponding to each straight line increases, whereas at high temperatures the plots show a maximum (Figure 3, top). The same behavior is observed in relation to the slope absolute error and the slope value (Figure 3, bottom).

The apparent isokinetic temperature decreases continuously as the dispersion factor increases at all temperatures (Figure 4). Both the intercept (Figure 5, top) and the slope (Figure 5, middle) of the enthalpy-entropy compensation straight lines increase as the correlation coefficient associated with the fit increases.

An interesting result is that the apparent isokinetic temperature (T_{ik}) is almost coincidental with the mean experimental temperature (T_m) when either its absolute error approaches zero (Figure 3, bottom), the dispersion factor equals zero (Figure 4) or the correlation coefficient is close to unity (Figure 5, middle). As a consequence, both the ratio T_{ik}/T_m and the correlation coefficient tend to unity simultaneously (Figure 5, bottom). This result is coherent with the predictions inferred from statistical studies.⁷⁻¹⁰

Results: Effect of Other Parameters. The influence of the magnitude of the experimental errors on the properties of the enthalpy-entropy compensation straight lines derived from laboratory uncertainties has been studied by a systematic change of the experimental error coefficient (Q), its increase resulting in an increase of both the apparent isokinetic temperature (Figure 6, top), approaching asymptotically the value corresponding to the mean experimental temperature:

$$\lim_{Q \rightarrow \infty} T_{ik} = T_m \quad (7)$$

and the correlation coefficient (Figure 6, bottom), approaching asymptotically the value corresponding to a perfect linear relationship:

$$\lim_{Q \rightarrow \infty} r = 1 \quad (8)$$

The next parameter systematically changed has been the experimental temperature range, that is, the difference between the maximum and minimum temperatures (ΔT) for the experimental interval chosen to perform the determination of the activation parameters. In this case, a decrease of ΔT leads to an increase of both the apparent isokinetic temperature (Figure 7, top), reaching the limit:

$$\lim_{\Delta T \rightarrow 0} T_{ik} = T_m \quad (9)$$

and the correlation coefficient (Figure 7, bottom), approaching asymptotically the value:

$$\lim_{\Delta T \rightarrow 0} r = 1 \quad (10)$$

The last parameters systematically changed have been the mean activation enthalpy and entropy. The results indicate that, keeping the other parameters constant, the apparent

isokinetic temperature increases when either $\Delta H_{\neq,m}^0$ decreases (Figure 8, top) or $\Delta S_{\neq,m}^0$ increases (Figure 8, bottom).

Comparison between the Different Effects. The apparent isokinetic temperatures for the enthalpy-entropy compensation straight lines derived from the numerical simulations performed have been plotted against the corresponding correlation coefficients. These curves were done by varying systematically one parameter each time and keeping all the others constant. A notable result is that the same curve is found whether the parameter changed was F , Q (Figure 9, top) or ΔT (Figure 9, bottom). However, the same cannot be stated when the parameter varied was either $\Delta H_{\neq,m}^0$ or $\Delta S_{\neq,m}^0$, since different plots are obtained in these cases (Figure 10).

Error-Driven Compensation Plots. It is interesting to draw attention to how a variation of the different parameters affects the linearity of the enthalpy-entropy compensation relationships derived solely from experimental errors. According to the numerical simulations performed, the correlation coefficient increases when either F decreases, Q increases, ΔT decreases, $\Delta H_{\neq,m}^0$ decreases or $\Delta S_{\neq,m}^0$ increases. Thus, an important result is that the linearity of the compensation line increases both when the magnitude of the experimental errors increases and when the interval between the maximum and minimum experimental temperatures decreases.

This is logical indeed, because it has been assumed as an initial hypothesis that there is no real correlation between the activation enthalpies and entropies of the members of the homologous reaction series (in Nature), so that the relationships found in the laboratory must necessarily come from the experimental errors. It can then be concluded that the confidence that is to be attributed to a compensation straight line observed in a certain kinetic research (in

the sense that it seems to be caused by a physically meaningful phenomenon) should improve when the experimental errors committed in the determination of the rate constants are as low as possible and when the experimental temperature range is as wide as possible.

5. *p*-Test

The main objective of the present work is that of developing a test designed to differentiate those isokinetic relationships with an experimental error origin from those caused by a physically meaningful phenomenon. Effectively, it has been observed in Figure 2 that an enthalpy-entropy compensation effect is found even when there is no real correlation between the activation parameters, provided that the accidental errors associated with the determination of the rate constants are high enough. Although some authors have published useful tools for this purpose,^{4,23,24} the search for a different alternative, potentially providing further quantitative information, seems attractive enough. Thus, the following goal of this research will be the elaboration of a test capable of discerning whether a certain activation enthalpy-entropy linear relationship found in the laboratory can be explained by the occurrence of experimental errors or not.

Several couples of parameters can be used as the basic framework of the desired test, such as the intercept of the compensation straight line and its corresponding absolute error (Figure 3, top) or the slope and its associated error (Figure 3, bottom). However, given the experimental information usually provided in the chemical literature, the parameters selected for this purpose have been the apparent isokinetic temperature (slope) and the correlation

coefficient of the enthalpy-entropy compensation linear fit. In the graphical version of the test, three different kinds of information will be represented in the $T_{ik} - r$ plane: i) the curve corresponding to the maximum probability of finding the points when the compensation straight line is caused exclusively by laboratory errors ($N = \infty$), ii) the points obtained from numerical simulations performed with the same number of reactions in the homologous series than in the real case ($N = N_{exp}$), and iii) the experimental point.

Maximum Probability Curve. The first step to develop the test will be the calculation of the $T_{ik} - r$ curve corresponding to the maximum probability. For that purpose, it would be required to perform the computer simulations with an infinite ensemble of reactions in the homologous series. However, since this would certainly be impossible, the simulations have been performed with $N = 10^5$ as a good enough approximation.

Due to the high number of parameters involved in the numerical simulations (T_m , ΔT , $\Delta H_{\neq, m}^0$, $\Delta S_{\neq, m}^0$, F , Q and N) and, consequently, of the different combinations to be considered, it is important to establish which of them can be kept constant and which should be varied. It has been shown that the $T_{ik} - r$ curve depends on the value of the mean experimental temperature (Figure 5, middle). Although this dependence is clearly weakened by using as ordinate the ratio T_{ik}/T_m instead, the suppression of that dependence is only partial because the resulting curves are still dependent on the value of T_m (Figure 5, bottom). The $T_{ik} - r$ plots also depend on the values of the mean activation parameters (Figure 10). Therefore, the mean value of the experimental temperature (T_m), as well as those of the activation enthalpy ($\Delta H_{\neq, m}^0$) and entropy ($\Delta S_{\neq, m}^0$), have to be specified for each reaction family.

Parameters F (measuring the dispersion of the real activation parameters) and Q (measuring the maximum limit of the experimental errors) should be employed as variables

because, in general, the chemical kinetics bibliography does not contain any information on their values. However, since it has been demonstrated that the $T_{ik} - r$ curve obtained by variation of parameter Q is coincident with that found when F was varied (Figure 9, top), an increase of the former being equivalent to a decrease of the latter, it will be enough if only one of those parameters is changed. The same happens with ΔT (Figure 9, bottom), its increase being equivalent to an increase of F and to a decrease of Q .

Calculation of the Probability Parameter. It can be observed that the dispersion of the activation parameters as measured in the laboratory (Figure 2, blue points) is higher than that associated with the real values as existing in Nature (Figure 2, purple points). This is so because the experimental determinations include not only the real dispersion of the activation parameters, but also the scattering caused by the accidental errors. Hence, the maximum limit that can be taken for the variable parameter F should be obtained for a situation of absence of experimental errors ($Q = 0$). Thus, in full coherence with eqs 2 and 3, it can be deduced from the activation enthalpies and entropies determined in the laboratory by means of the following equation:

$$F_{\max} = 10 \frac{(|\Delta X_{\neq, i}^o - \Delta X_{\neq, m}^o|)_{\max}}{\Delta X_{\neq, m}^o} \quad (11)$$

where $X = H$ or S . This limit can be calculated from the highest absolute value of the difference between the individual ($\Delta X_{\neq, i}^o$) and mean ($\Delta X_{\neq, m}^o$) activation parameters for the homologous reaction series considered.

The values allowed for the dispersion factor will be in the range $0 \leq F \leq F_{\max}$. The lower limit ($F = 0$) corresponds to a situation in which the activation parameters are identical for all the members of the homologous reaction series and the experimental dispersion is thus completely due to accidental errors ($Q = F_{\max}$), whereas the upper limit ($F = F_{\max}$) corresponds to a situation in which the real dispersion of the activation parameters is identical to the one experimentally observed due to the absence of errors ($Q = 0$). Therefore, the values of parameter Q will obey the following equation:

$$Q = F_{\max} - F \quad (12)$$

so that, as parameter F increases from 0 to F_{\max} , parameter Q decreases from F_{\max} to 0. The values of the other parameters will be taken as done for the maximum probability curve except the number of reactions involved in the simulated homologous series, being now equal to that of the experimental case ($N = N_{\text{exp}}$).

Given that the number of reactions studied in each homologous family is indeed much lower than that required to obtain the maximum probability curve ($N = 10^5$), when the numerical simulations are done with $N = N_{\text{exp}}$ and represented in a graphic the points will appear scattered above and below that curve. The objective of the test will be, precisely, to determine the probability of finding one of these simulation points in a region of the $T_{\text{ik}} - r$ plane near the experimental point.

Although none of the simulations will be exactly coincident with the empirical situation, some of them will potentially lead to points placed close enough: the higher the distance between the experimental point and the maximum probability curve, the lower the probability

of finding a simulation point in its vicinity. At this moment, there are two different ways to continue with the calculations. The simpler would be to accept as valid those simulations leading to results contained in certain ranges around $(T_{ik})_{exp}$ and r_{exp} . However, the limitation inherent to this procedure would be the choice of the range widths, since an increase of the region area would automatically result in an increase of the corresponding probability. In order to outline the second alternative, one must wonder why the experimental point is not exactly placed on the maximum probability curve. Only two alternative explanations are possible: i) the number of members in the reaction series is too low ($N_{exp} \ll \infty$) and ii) the hypothesis based on which the numerical simulations were performed (no real correlation between the family activation parameters) is wrong.

Therefore, the chance of the compensation linear plot being originated by accidental errors will be lower when the experimental point is placed far from the maximum probability curve, either above or below it. However, as mentioned before, it is impossible to find a simulation exactly matching the empirical information obtained from the bibliography:

$$(T_{ik})_{sim} \neq (T_{ik})_{exp} \quad (13)$$

$$r_{sim} \neq r_{exp} \quad (14)$$

Once assumed this, it is important to define which simulations will be taken as valid (capable of explaining the experimental isokinetic correlation) and which ones will not:

All the simulations leading to points located farther from the maximum probability curve (as concerning the apparent isokinetic temperature) than the experimental point should be considered as valid, provided that the associated correlation coefficient is high enough.

This condition derives from the fact that the probability of finding a particular (T_{ik}, r) couple of values is inversely proportional to its distance with respect to the curve of maximum probability, obtained the latter from simulations performed with a value of parameter N (the number of members belonging to the homologous reaction series) as high as possible. It is thus clear that all the simulations, performed with a number of members of the homologous reaction series $N = N_{exp}$, leading to apparent isokinetic temperatures with at least the same difference (in absolute value) from the slope predicted by the maximum probability curve than that corresponding to the experimental enthalpy-entropy compensation straight line are, in principle, capable of explaining the information found in the laboratory. Only those simulations leading to correlation coefficients too low in comparison with the experimental one should be excluded.

Hence, the test will count the number of simulation points in the $T_{ik} - r$ plane fulfilling the following criteria:

$$|(T_{ik})_{sim} - (T_{ik})_{cmp}| \geq |(T_{ik})_{exp} - (T_{ik})_{cmp}| \quad (15)$$

$$r_{sim} \geq r_{exp} \quad (16)$$

where the subscripts indicate whether the slope and the correlation coefficient of the enthalpy-entropy compensation linear plots correspond to either the numerical simulation with $N = N_{\text{exp}}$ (sim), the curve of maximum probability with $N = 10^5$ (cmp) or the experimental homologous series (exp). The value of $(T_{\text{ik}})_{\text{cmp}}$ is calculated as that belonging to the curve with the abscissa $r = r_{\text{exp}}$.

Because of the use of absolute values in eq 15, the only simulations regarded as capable of explaining the laboratory kinetic data will be those leading to isokinetic temperatures higher than or equal to the experimental value $[(T_{\text{ik}})_{\text{sim}} \geq (T_{\text{ik}})_{\text{exp}}]$ when the point is placed above the maximum probability curve $[(T_{\text{ik}})_{\text{exp}} > (T_{\text{ik}})_{\text{cmp}}]$, and to isokinetic temperatures lower than or equal to the experimental value $[(T_{\text{ik}})_{\text{sim}} \leq (T_{\text{ik}})_{\text{exp}}]$ when the point is placed below the maximum probability curve $[(T_{\text{ik}})_{\text{exp}} < (T_{\text{ik}})_{\text{cmp}}]$. Moreover, in order for the numerical simulations to be considered as valid, it will be required that the corresponding correlation coefficient be higher than or equal to the experimental one (eq 16).

The final output of the test consists in calculating the probability of the enthalpy-entropy compensation straight line being explainable by accidental errors as:

$$p = \frac{n [(T_{\text{ik}})_{\text{sim}} \geq (T_{\text{ik}})_{\text{exp}}, r_{\text{sim}} \geq r_{\text{exp}}]}{n_{\text{T}}} \quad (17)$$

$$p = \frac{n [(T_{\text{ik}})_{\text{sim}} \leq (T_{\text{ik}})_{\text{exp}}, r_{\text{sim}} \geq r_{\text{exp}}]}{n_{\text{T}}} \quad (18)$$

where the numerators are the numbers of simulations fulfilling the conditions imposed by eqs 15 and 16, whereas the symbol appearing in the denominators stands for the total number of

simulations performed with $N = N_{\text{exp}}$. It should be noticed that eq 17 is used when $(T_{\text{ik}})_{\text{exp}} > (T_{\text{ik}})_{\text{cmp}}$ and eq 18 when $(T_{\text{ik}})_{\text{exp}} < (T_{\text{ik}})_{\text{cmp}}$.

Application to Bibliographic Data. The occurrence of activation enthalpy-entropy compensation plots for different homologous reaction series is rather ubiquitous in the chemical kinetics literature. The p -test developed in the present work has been used to calculate the value of the probability (p) of finding a numerical simulation able to explain the observation of a particular enthalpy-entropy compensation relationship just as a consequence of experimental errors. Therefore, parameter p measures the probability that a certain isokinetic plot might accept an accidental-error explanation (error-driven isokinetic plot). The application of the p -test to three bibliography cases,^{1,25,26} two with the experimental points above the maximum probability curve [$(T_{\text{ik}})_{\text{exp}} > (T_{\text{ik}})_{\text{cmp}}$] and the other below [$(T_{\text{ik}})_{\text{exp}} < (T_{\text{ik}})_{\text{cmp}}$] is illustrated in Figure 11. It can be observed that in the first case there is no simulation that could be considered as valid, whereas in the other two cases some simulations actually fulfilled the conditions imposed by eqs 17 and 18.

The p -test has been applied to 100 different homologous reaction series taken from the chemical literature.^{1,4,25-89} A very high number ($n_{\text{T}} = 10^6$) of numerical simulations were done in each case in order to obtain an accurate value of parameter p . The complete results are shown in Table S1 (Supporting Information), and those corresponding to the reaction series with a notably high likelihood of presenting a physically meaningful compensation effect ($p \leq 0.000025$) in Table 2. In four series the probability could not be obtained because of its extremely low value ($p < 10^{-6}$). Moreover, the condition of statistical significance (usually accepted as $p < 0.05$) was fulfilled for 63 homologous series, not being reached that level of significance in the other 37 cases. It can then be concluded that many of the isokinetic plots

found in the bibliography (probably, more than 50%) are difficult to be explained just as a consequence of accidental errors, so that a real activation enthalpy-entropy correlation has to be necessarily postulated for those reaction families.

Although parameter p is a function of several variables (N_{exp} , F_{max} , $T_{\text{ik}}/T_{\text{m}}$ and r), the only one capable of predicting with some accuracy its value is the correlation coefficient of the experimental isokinetic plot, thus denoting a stronger influence than those of the other three variables. As shown in Figure 12 (top), an increase of the correlation coefficient results in a net decrease of the probability parameter. This means that the higher the linearity of the activation enthalpy-entropy compensation plot the lower the probability that it could be explained by accidental errors.

An attempt has been made to elucidate the combined effect of the four independent factors on the probability parameter. A reasonably linear relationship (Figure 12, bottom) was found when representing $\log (1 - p)$ against the following variable:

$$\log z = a \log N_{\text{exp}} + b \log F_{\text{max}} + c \log \left(\frac{T_{\text{ik}}}{T_{\text{m}}} \right) + \log r \quad (19)$$

where $a = 0.0508$, $b = 0.0204$ and $c = 0.0738$ quantify the statistical weight of each factor with respect to that of the correlation coefficient (arbitrarily taken as 1). These parameters were obtained by systematically changing their values in order to minimize the sum of the absolute errors of the individual points with respect to the linear relationship considered as the best fit. The fact that $a, b, c \ll 1$ confirms the outstanding influence of r in comparison with those of N_{exp} , F_{max} and $T_{\text{ik}}/T_{\text{m}}$, although the four of them have a positive effect on the value of $1 - p$. This indicates that a certain isokinetic plot should be regarded as more physically

meaningful (with a lower chance to be an artefact resulting from experimental errors) when the values of these four magnitudes are as high as possible.

Two interesting examples are shown in Figure 13, corresponding to the oxidations of substituted alkenes by permanganate ion in water⁴¹ and by quaternary ammonium permanganate in dichloromethane.¹ In both cases the isokinetic temperature is higher than the mean experimental temperature ($T_{ik} / T_m > 1$) and both can be considered as statistically significant ($p = 0.000197$ and $< 10^{-6}$, respectively).

The present work can be considered as a *reductio ad absurdum* argument: starting as an initial hypothesis that the activation enthalpy-entropy parameters for all the homologous series are randomly scattered in Nature, the final conclusion is that (at least for some reaction families) it cannot be true, since a pre-existing correlation must actually be postulated to explain the experimental data.

Several methods have been previously proposed to discriminate error-induced compensation plots from those with a real physical origin.^{3,4,23,24,90,91} These methods can be regarded as complementary, often leading to coherent results. However, the one now presented (p -test) might be more intuitive, because it yields a parameter with a direct physical interpretation: the probability of an isokinetic relationship found for a particular homologous reaction series being explainable as a consequence of random experimental errors.

6. ASSOCIATED CONTENT

Supporting Information

The Supporting Information is available free of charge on the [ACS Publications website](#).

. Parameters involved in the application of the p -test to different experimental isokinetic plots extracted from the bibliography (Table S1). BASIC-language computer program for the determination of the probability of a particular enthalpy-entropy compensation plot being caused by accidental errors (p -test).

7. AUTHOR INFORMATION

Corresponding Author

* E-mail: jfperezdebenito@ub.edu. Tel: 34 93 4020473. Fax: 34 93 4021231.

Notes

The authors declare no competing financial interest.

8. REFERENCES

- (1) Perez-Benito, J. F. Substituent Effects on the Oxidation of Cinnamic Acid by Methyltributylammonium Permanganate in Methylene Chloride. *Chem. Scr.* **1987**, 27, 433–436.
- (2) Pan, A.; Biswas, T.; Rakshit, A. K.; Moulik, S. P. Enthalpy-Entropy Compensation (EEC) Effect: A Revisit. *J. Phys. Chem. B* **2015**, 119, 15876–15884.
- (3) Petersen, R. C.; Markgraf, J. H.; Ross, S. D. Solvent Effects in the Decomposition of 1,1'-Diphenylazoethane and 2,2'-Azobis-(2-methylpropionitrile). *J. Am. Chem. Soc.* **1961**, 83, 3819–3823.

- (4) Wiberg, K. B. *Physical Organic Chemistry*; Wiley: New York, 1964.
- (5) Leffler, J. E. The Enthalpy-Entropy Relationship and Its Implications for Organic Chemistry. *J. Am. Chem. Soc.* **1955**, *20*, 1202–1231.
- (6) Perez-Benito, J. F. Some Tentative Explanations for the Enthalpy-Entropy Compensation Effect in Chemical Kinetics: From Experimental Errors to the Hinshelwood-Like Model. *Monatsh. Chem.* **2013**, *144*, 49–58.
- (7) Krug, R. R.; Hunter, W. G.; Grieger R. A. Statistical Interpretation of Enthalpy-Entropy Compensation. *Nature*. **1976**, *261*, 566–567.
- (8) Krug, R. R.; Hunter, W. G.; Grieger R. A. Enthalpy-Entropy Compensation. 1. Some Fundamental Statistical Problems Associated with the Analysis of van't Hoff and Arrhenius Data. *J. Phys. Chem.* **1976**, *80*, 2335–2341.
- (9) Krug, R. R.; Hunter, W. G.; Grieger R. A. Enthalpy-Entropy Compensation. 2. Separation of the Chemical from the Statistical Effect. *J. Phys. Chem.* **1976**, *80*, 2341–2351.
- (10) Lente, G.; Fabian, I.; Poe, A. J. A Common Misconception about the Eyring Equation. *New J. Chem.* **2005**, *29*, 759–760.
- (11) Sharp, K. Enthalpy-Entropy Compensation: Fact or Artifact? *Prot. Sci.* **2001**, *10*, 661–667.
- (12) Cornish-Bowden, A. Enthalpy-Entropy Compensation: A Phantom Phenomenon. *J. Biosci.* **2002**, *27*, 121–126.
- (13) Lei, L.; Guo, Q. X. Isokinetic Relationship, Isoequilibrium Relationship, and Enthalpy-Entropy Compensation. *Chem. Rev.* **2001**, *101*, 673–695.
- (14) Larsson, R. Concluding Remarks on the Theory of Selective Energy Transfer and Exemplification on a Zeolite Kinetics Study. *Monatsh. Chem.* **2013**, *144*, 21–28.

- (15) Yelon, A.; Sacher, E; Linert, W. Multi-Excitation Entropy, Entropy-Enthalpy Relations, and Their Impact on Catalysis. *Catal. Lett.* **2011**, *141*, 954–957.
- (16) Koudrtiavtsev, A. B.; Linert, W. Isokinetic and Isoequilibrium Relationships in the Gaseous Phase. *Monatsh. Chem.* **2013**, *144*, 29–40.
- (17) Moyano, P. C.; Zuñiga, R. N. Enthalpy-Entropy Compensation for Browning of Potato Strips during Deep-Fat Frying. *J. Food. Eng.* **2004**, *63*, 57–62.
- (18) Movileanu, L.; Schiff, E. A. Entropy-Enthalpy Compensation of Biomolecular Systems in Aqueous Phase: A Dry Perspective. *Monatsh. Chem.* **2013**, *144*, 59–65.
- (19) Crine J. P. The Compensation Law in Dielectric Polymer Relaxation. *Monatsh. Chem.* **2013**, *144*, 11–19.
- (20) Engstrom, O. Compensation Effects at Electron Traps in Semiconductors. *Monatsh. Chem.* **2013**, *144*, 73–82.
- (21) Abdel-Wahab, F.; Montaser, A. A.; Yelon, A. Mechanism of ac and dc Conduction in Chalcogenide Glasses. *Monatsh. Chem.* **2013**, *144*, 83–89.
- (22) Barlow, R. *Statistics: A Guide to the Use of Statistical Methods in the Physical Sciences*; Wiley: New York, 1989.
- (23) Vlasov. V. M. Varying the Activation Parameters as a Method of Determining whether There Is an Isokinetic Relationship among the Bimolecular Nucleophilic Reactions of Benzene Derivatives in Solution. *Monatsh. Chem.* **2013**, *144*, 41–48.
- (24) Vlasov. V. M. Effects of Substituents on Activation Parameter Changes in the Michael-Type Reactions of Nucleophilic Addition to Activated Alkenes and Alkynes in Solution. *Monatsh. Chem.* **2016**, *147*, 319–328.
- (25) Branch, G. E. K.; Nixon, A. C. The Rates of Alcoholysis of Acyl Chlorides. *J. Am. Chem. Soc.* **1936**, *58*, 2499–2504.

- (26) Oh, H. K.; Yang, J. H.; Sung, D. D.; Lee, I. Kinetics and Mechanism of the Addition of Benzylamines to β -Nitrostyrenes in Acetonitrile. *J. Chem. Soc., Perkin Trans. 2* **2000**, 101–105.
- (27) Keane, M. A.; Larsson, R. Isokinetic Behaviour in Gas Phase Catalytic Haloarene Hydrodehalogenation Reactions: Mechanistic Considerations. *J. Mol. Catal. A Chem.* **2006**, 249, 158–165.
- (28) Keane, M. A.; Larsson, R. Isokinetic Behaviour in Gas Phase Catalytic Hydrodechlorination of Chlorobenzene over Supported Nickel. *J. Mol. Catal. A Chem.* **2007**, 268, 87–94.
- (29) Abu-Gharib, E. A.; El-Khatib, R. M.; Nassr, L. A. E.; Abu-Dief, A. M. Reactivity Trends in the Base Hydrolysis of 6-Nitro-2H-chromen-2-one and 6-Nitro-2H-chromen-2-one-3-carboxylic Acid in Binary Mixtures of Water with Methanol and Acetone at Different Temperatures. *Kinet. Catal.* **2012**, 53, 182–187.
- (30) Nikolic, J. B.; Uscumlic, G. S. Solvent and Structural Effects on the Activation Parameters of the Reaction of Carboxylic Acids with Diazodiphenylmethane. *Int. J. Chem. Kinet.* **2013**, 45, 256–265.
- (31) Berliner, E.; Altschul, L. The Hydrolysis of Substituted Benzoic Anhydrides. *J. Am. Chem. Soc.* **1952**, 74, 4110–4113.
- (32) Overberger, C. G.; Cummins, R. W. Mechanism of the Oxidation of *p,p'*-Dichlorobenzyl Sulfide by Peroxybenzoic and *para* Substituted Peroxybenzoic Acids. *J. Am. Chem. Soc.* **1953**, 75, 4250–4254.
- (33) Cafferata, L. F. R.; Eyler, G. N.; Svartman, E. L.; Cañizo, A. I.; Alvarez, E. Solvent Effects in the Thermal Decomposition Reactions of Cyclic Ketone Diperoxides. *J. Org. Chem.* **1991**, 56, 411–414.

- (34) Shpanko, I. V.; Sadovaya, I. V. Isoparametricity Phenomenon and Kinetic Enthalpy-Entropy Compensation Effect: Experimental Evidence Obtained by Investigating Pyridine-Catalyzed Reactions of Phenyloxirane with Benzoic Acids. *Kinet. Catal.* **2014**, *55*, 56–63.
- (35) Vanzin, D.; Fiori, S.; Biondo, P. B. F.; Feltrim, G.; Gracetto, A. C.; Tessaro, A. L.; Politi, M. J.; Caetano, W.; Hioka, N. Microenvironment Effects on the Kinetics of the Alkaline Hydrolysis of Bispyridinium Conformers. *Int. J. Chem. Kinet.* **2013**, *45*, 703–711.
- (36) Cantwell, N. H.; Brown, E. V. Effect of Solvents on the Decarboxylation of Picolinic Acid. *J. Am. Chem. Soc.* **1953**, *75*, 4466–4468.
- (37) Blomquist, A. T.; Bernstein, I. A. The Kinetics of the Thermal Decomposition of Peresters. III. The Effect of *p*-Substituents on the Unimolecular Decomposition of *t*-Butyl Perbenzoates. *J. Am. Chem. Soc.* **1951**, *73*, 5546–5550.
- (38) Cross, R. P.; Fugassi, P. The Kinetics of Semicarbazone Formation with Para Substituted Acetophenones. *J. Am. Chem. Soc.* **1949**, *71*, 223–225.
- (39) Meloche, I.; Laidler, K. J. Substituent Effect in the Acid and Base Hydrolyses of Aromatic Amides. *J. Am. Chem. Soc.* **1951**, *73*, 1712–1714.
- (40) Shpanko, I. V.; Sadovaya, I. V. Joint Effect of Structure and Temperature on the Rates of the Reactions of 3,5-Dinitrophenyloxirane with Arenesulfonic Acids: Compensation Effect and Isoparametricity. *Kinet. Catal.* **2011**, *52*, 647–653.
- (41) Wiberg, K. B.; Geer, R. D. The Kinetics of the Permanganate Oxidation of Alkenes. *J. Am. Chem. Soc.* **1966**, *88*, 5827–5832.
- (42) Bratlie, K. M.; Li, Y.; Larsson, R.; Somorjai, G. A. Compensation Effect of Benzene Hydrogenation on Pt(111) and Pt(100) Analyzed by the Selective Energy Transfer Model. *Catal. Lett.* **2008**, *121*, 173–178.

- (43) Laksmi, B.; Shivananda, K. N.; Puttaswamy; Mahendra, K. N.; Gowda, N. M. M.; Jagadeesh, R. V. An Efficient Platinum-Catalyzed Oxidation Process and Mechanism for the Facile Conversion of Benzoxazoles to Aminophenols. *Chem. Eng. J.* **2010**, *163*, 403–412.
- (44) Gupta, K. K. S.; Pal, B.; Sen, P. K. Kinetics and Mechanism of the Oxidation of Some α -Hydroxy Acids by Tetrachloroaurate(III) in Acetic Acid-Sodium Acetate Buffer Medium. *Int. J. Chem. Kinet.* **1999**, *31*, 873–883.
- (45) Alder, M. G.; Leffler, J. E. The Role of the Solvent in Radical Decomposition Reactions: Phenylazotriphenylmethane. *J. Am. Chem. Soc.* **1954**, *76*, 1425–1427.
- (46) Newman, M. S.; Lee, S. H.; Garrett, A. B. Solvent Effect in the Curtius Rearrangement of Benzazide. *J. Am. Chem. Soc.* **1947**, *69*, 113–116.
- (47) Morse, B. K.; Tarbell, D. S. Cleavage of the Carbon-Sulfur Bond. Rates of the Basic and the Acid-Catalyzed Hydrolysis of Allyl, Benzyl and Trityl Thioacetates, and the Corresponding Acetates in Aqueous Acetone Solution. *J. Am. Chem. Soc.* **1952**, *74*, 416–419.
- (48) Tarasow, T. M.; Hilvert, D. Investigation of Medium Effects in a Family of Decarboxylase Antibodies. *J. Am. Chem. Soc.* **1994**, *116*, 7959–7963.
- (49) Croce, L. J.; Gettler, J. D. The Benzidine Rearrangement. Kinetics and Temperature Coefficients of the Rearrangements of Hydrazobenzene and Certain Substituted Hydrazobenzenes. *J. Am. Chem. Soc.* **1953**, *75*, 874–879.
- (50) Keane, M. A.; Larsson, R. Application of the Selective Energy Transfer Model to Account for an Isokinetic Response in the Gas Phase Reductive Cleavage of Hydroxyl, Carbonyl and Carboxyl Groups from Benzene over Nickel/Silica. *Catal. Lett.* **2009**, *129*, 93–103.

- (51) Ivanov, S. N.; Mikhailov, A. V.; Gnedin, B. G.; Lebedukho, A. Y.; Korolev, V. P. Solvation Bifunctional Catalysis of the Hydrolysis of Sulfonyl Chlorides by Hydration Complexes of 2-Propanol: Influence of the Substrate Structure. *Kinet. Catal.* **2005**, *46*, 35–43.
- (52) Hackett, J. W.; Thomas, H. C. Exchange Reaction and Hydrolysis of *p*-Nitrobenzyl Bromide in Dioxane-Water Solutions. *J. Am. Chem. Soc.* **1950**, *72*, 4962–4964.
- (53) Smith, H. A.; Burn, J. Kinetics of the Acid-Catalyzed Esterification of Phenyl- and Cyclohexyl-Substituted Aliphatic Acids in Methanol. *J. Am. Chem. Soc.* **1944**, *66*, 1494–1497.
- (54) Morgan, M. S.; Cretcher, L. H. A Kinetic Study of Alkylation by Ethyl Arylsulfonates. *J. Am. Chem. Soc.* **1948**, *70*, 375–378.
- (55) Price, C. C.; Lincoln, D. C. The Rates of Saponification of Some Ortho-Substituted Ethyl *m*- and *p*-Aminobenzoates. *J. Am. Chem. Soc.* **1951**, *73*, 5838–5841.
- (56) Cristol, S. J.; Hause, N. L.; Meek, J. S. Mechanisms of Elimination Reactions. III. The Kinetics of the Alkaline Dehydrochlorination of the Benzene Hexachloride Isomers. II. *J. Am. Chem. Soc.* **1951**, *73*, 674–679.
- (57) Miller, S. I.; Noyes, R. M. Kinetics of Basic Elimination Reactions of the Dihaloethylenes and the Mechanism of *trans* Elimination. *J. Am. Chem. Soc.* **1952**, *74*, 629–636.
- (58) Waring, C. E.; Abrams, J. R. Some Kinetic Considerations of the Thermal Decomposition of Benzenediazonium Chloride in Various Solvents. *J. Am. Chem. Soc.* **1941**, *63*, 2757–2762.
- (59) Shen, Y.; Moss, R. A.; Krogh-Jespersen, K. Directly Measured Activation Parameters for the Ring Expansions of Cyclopropylhalocarbenes. *J. Am. Chem. Soc.* **2012**, *3*, 910–913.

- (60) Karunakaran, C.; Chidambaranathan, V. Linear Free Energy Relationships near Isokinetic Temperature. Oxidation of Organic Sulfides with Nicotinium Dichromate. *Croat. Chem. Acta* **2001**, *74*, 51–59.
- (61) Bustillo, S.; Leiva, L. C.; Jorge, N. L.; Gomez, M. E.; Castro, E. A. Solvent Effects in the Thermal Decomposition Reactions of Cyclic Benzaldehyde Diperoxide. *Trends Appl. Sci. Res.* **2006**, *1*, 640–644.
- (62) Cristol, S. J.; Begoon, A. Mechanisms of Elimination Reactions. VII. The Alkaline Dehydrohalogenation of Chloro- and Bromo-Maleate and Fumarate. *J. Am. Chem. Soc.* **1952**, *74*, 5025–5029.
- (63) Cristol, S. J.; Barasch, W. Mechanisms of Elimination Reactions. IV. Effect of Solvent Composition on the Kinetics of Dehydrochlorination of Benzene Hexachloride Isomers in Aqueous Ethanol. *J. Am. Chem. Soc.* **1952**, *74*, 1658–1660.
- (64) Badin, E. J.; Pacsu, E. Kinetics and Mechanism of the Acid Catalyzed Racemization of (+)2-Methyl-butanol-1. *J. Am. Chem. Soc.* **1945**, *67*, 1353–1356.
- (65) Craft, M. J.; Lester, C. T. Rate of Oxime Formation of Isomeric Ketones from *p*-Cymene. *J. Am. Chem. Soc.* **1951**, *73*, 1127–1128.
- (66) Rylander, P. N.; Tarbell, D. S. Cleavage of the Carbon-Sulfur Bond. Rates of Hydrolysis of Some Alkyl Acetates and the Corresponding Thiolacetates in Aqueous Acetone. *J. Am. Chem. Soc.* **1950**, *72*, 3021–3025.
- (67) Gonzalez, G.; Lahuerta, P.; Martinez, M.; Peris, E.; Sanau, M. Mechanism of the Acid-Catalyzed Cyclometallation Reaction of Dirhodium(II) Compounds with General Formula $[\text{Rh}_2(\text{O}_2\text{CMe})(\mu\text{-O}_2\text{CMe})_2\{(\text{C}_6\text{H}_4)\text{PPh}_2\}\{\text{P}(\text{C}_6\text{H}_4\text{X})\}_3](\text{OH}_2)]$. *J. Chem. Soc., Dalton Trans.* **1994**, *4*, 545–550.

- (68) Brown, W. G.; Fried, S. Steric Factors in Quaternary Salt Formation. *J. Am. Chem. Soc.* **1943**, *65*, 1841–1845.
- (69) Pavez, P.; Millan, D.; Rojas, M.; Morales, J. I.; Santos, J. G. Reaction Mechanism in Ionic Liquids: Kinetics and Mechanism of the Aminolysis of 4-Nitrophenyl Acetate. *Int. J. Chem. Kinet.* **2016**, *48*, 337–343.
- (70) Heidt, L. J.; Purves, C. B. Thermal Rates and Activation Energies for the Aqueous Acid Hydrolysis of α - and β -Methyl, Phenyl and Benzyl-D-glucopyranosides, α - and β -Methyl and β -Benzyl-D-fructopyranosides, and α -Methyl-D-fructofuranoside. *J. Am. Chem. Soc.* **1944**, *66*, 1385–1389.
- (71) Nakamura, T.; Busfield, W. K.; Jenkins, I. D.; Rizzardo, E.; Thang, S. H.; Suyama, S. Thermal Decomposition Mechanisms of *tert*-Alkyl Peroxypivalates Studied by the Nitroxide Radical Trapping Technique. *J. Org. Chem.* **2000**, *65*, 16–23.
- (72) Hartman, R. J.; Hoogsteen, H. M.; Moede, J. A. The Kinetics of the Hydrion Catalyzed Esterification of Some Substituted Benzoic Acids with Cyclohexanol. *J. Am. Chem. Soc.* **1944**, *66*, 1714–1718.
- (73) Nalwaya, N.; Jain, A.; Hiran, B. L. Oxidation of Some α -Amino Acids by Pyridinium Bromochromate in an Aquo-Acetic Acid Medium – A Kinetic and Mechanistic Study. *Kinet. Catal.* **2004**, *45*, 345–350.
- (74) Heidt, L. J.; Purves, C. B. The Unimolecular Rates of Hydrolysis of 0.01 Molar Methyl- and Benzylfructofuranosides and -Pyranosides and of Sucrose in 0.00965 Molar Hydrochloric Acid at 20 to 60°. *J. Am. Chem. Soc.* **1938**, *60*, 1206–1210.
- (75) Noda, H. L.; Kuby, S. A.; Lardy, H. A. Properties of Thioesters: Kinetics of Hydrolysis in Dilute Aqueous Media. *J. Am. Chem. Soc.* **1953**, *75*, 913–917.

- (76) Beringer, F. M.; Sands, S. The Synthesis, Acidity and Decarboxylation of Substituted Mesitoic Acids. *J. Am. Chem. Soc.* **1953**, 75, 3319–3322.
- (77) Winstein, S.; Marshall, H. Neighboring Carbon and Hydrogen. VI. Formolysis and Other Solvolysis Rates of Some Simple Secondary and Primary Benzenesulfonates. *J. Am. Chem. Soc.* **1952**, 74, 1120–1126.
- (78) Oh, H. K.; Kim, I. K.; Sung, D. D.; Lee, I. Kinetics and Mechanism of Benzylamine Additions to Ethyl α -Acetyl- β -phenylacrylates in Acetonitrile. *Org. Biomol. Chem.* **2004**, 2, 1213–1216.
- (79) Blomquist, A. T.; Buselli, A. J. The Decomposition of *sym*-Substituted Benzoyl Peroxides. *J. Am. Chem. Soc.* **1951**, 73, 3883–3888.
- (80) Sauer, R. W.; Krieger, K. A. Catalytic Surfaces and the Hydrolysis of Diethyl Carbonate. *J. Am. Chem. Soc.* **1952**, 74, 3116–3120.
- (81) Nisar, J.; Awan, I. A. A Gas-Phase Kinetic Study on the Thermal Decomposition of 2-Chloropropene. *Kinet. Catal.* **2008**, 49, 461–465.
- (82) Swain, C. G.; Scott, C. B. Rates of Solvolysis of Some Alkyl Fluorides and Chlorides. *J. Am. Chem. Soc.* **1953**, 75, 246–248.
- (83) Dyas, H. E.; Hill, D. G. The Mutarotation of Glucose in Water-Methanol Mixtures. *J. Am. Chem. Soc.* **1942**, 64, 236–240.
- (84) Oh, H. K.; Kim, T. S.; Lee, H. W.; Lee, I. Kinetics and Mechanism of the Addition of Benzylamines to β -Nitrostilbenes and β -Cyano-4'-nitrostilbenes. *J. Chem. Soc., Perkin Trans. 2* **2002**, 282–286.
- (85) Brown, H. C.; Berneis, H. L. Steric Strains as a Factor in the Solvolytic Reactions of Neopentylidimethyl and Dineopentylmethylcarbonyl Chlorides. *J. Am. Chem. Soc.* **1953**, 75, 10–14.

- (86) Brown, H. C.; Borkowski, M. The Effect of Ring Size on the Rate of Solvolysis of the 1-Chloro-1-methylcycloalkanes. *J. Am. Chem. Soc.* **1952**, *74*, 1894–1902.
- (87) Oh, H. K.; Kim, I. K.; Lee, H. W.; Lee, I. Kinetics and Mechanism of the Addition of Benzylamines to Benzylienediethylmalonates in Acetonitrile. *J. Org. Chem.* **2004**, *69*, 3806–3810.
- (88) Moss, R. A.; Zhang, M. Activation Parameters for Additions of Ambiphilic Methoxychlorocarbene to Alkenes. *Org. Lett.* **2008**, *18*, 4045–4048.
- (89) Berliner, E.; Monack, L. C. Nucleophilic Displacement in the Benzene Series. *J. Am. Chem. Soc.* **1952**, *74*, 1574–1579.
- (90) Linert, W.; Soukup, R. W.; Schmid, R. Statistical Analysis of the Isokinetic Relationship Using a Programmable Calculator. *Comput. Chem.* **1982**, *6*, 47–55.
- (91) Linert, W. The Isokinetic Relationship. VII. Statistical Analyses and Examples for Unimolecular Reaction Systems. *Inorg. Chim. Acta* **1988**, *141*, 233–242.

Table 1. Effect of the Dispersion Factor on the Enthalpy-Entropy Compensation Plot

F	T_{ik} / K	r
0.00	297.5 ± 0.7	0.9997
0.25	272.2 ± 9.2	0.9487
0.50	237.6 ± 16.7	0.8210
0.75	200.4 ± 22.5	0.6685

^a F is the dispersion factor of the activation parameters (without experimental errors). ^b T_{ik} is the apparent isokinetic temperature. ^c r is the correlation coefficient associated with the enthalpy-entropy compensation plot.

Table 2. Application of the p -Test to Experimental Isokinetic Plots Extracted from the Bibliography with a High Probability of Being Physically Meaningful

Reference	N_{exp}	F_{max}	$T_{\text{ik}}/T_{\text{m}}$	r	p
1	13	2.64	2.19 ± 0.18	0.9644	$< 10^{-6}$
27	16	7.31	1.20 ± 0.03	0.9942	$< 10^{-6}$
28	10	7.72	1.29 ± 0.02	0.9990	$< 10^{-6}$
29	6	0.96	1.64 ± 0.03	0.9993	$< 10^{-6}$
30	12	5.40	1.32 ± 0.06	0.9909	0.000001
31	9	3.39	2.20 ± 0.26	0.9550	0.000002
32	7	4.06	1.50 ± 0.07	0.9941	0.000002
30	12	4.65	1.57 ± 0.11	0.9762	0.000009
33	8	26.9	1.17 ± 0.03	0.9983	0.000011
34	5	9.24	0.93 ± 0.01	0.9999	0.000022
29	6	1.03	1.65 ± 0.11	0.9913	0.000025

^a N_{exp} is the number of members of the homologous reaction series. ^b F_{max} is the maximum value of the dispersion factor of the activation parameters. ^c T_{ik} is the experimental isokinetic temperature. ^d T_{m} is the mean experimental temperature. ^e r is the correlation coefficient of the experimental isokinetic plot. ^f p is the probability of the isokinetic plot being explainable by accidental errors.

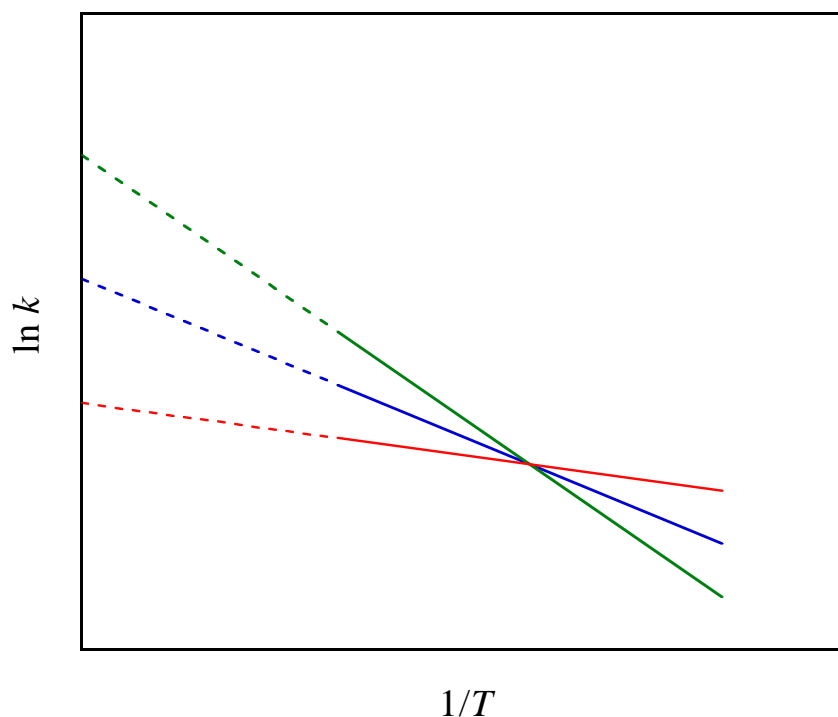


Figure 1. Qualitative representation illustrating how experimental errors affect the Arrhenius plots. The blue straight line corresponds to the real behavior of the process. The green line simulates the situation found when the errors associated with the higher temperatures are positive and those associated with the lower temperatures negative, whereas the red line shows the opposite case. The intercrossing point marks the position of the apparent isokinetic temperature.

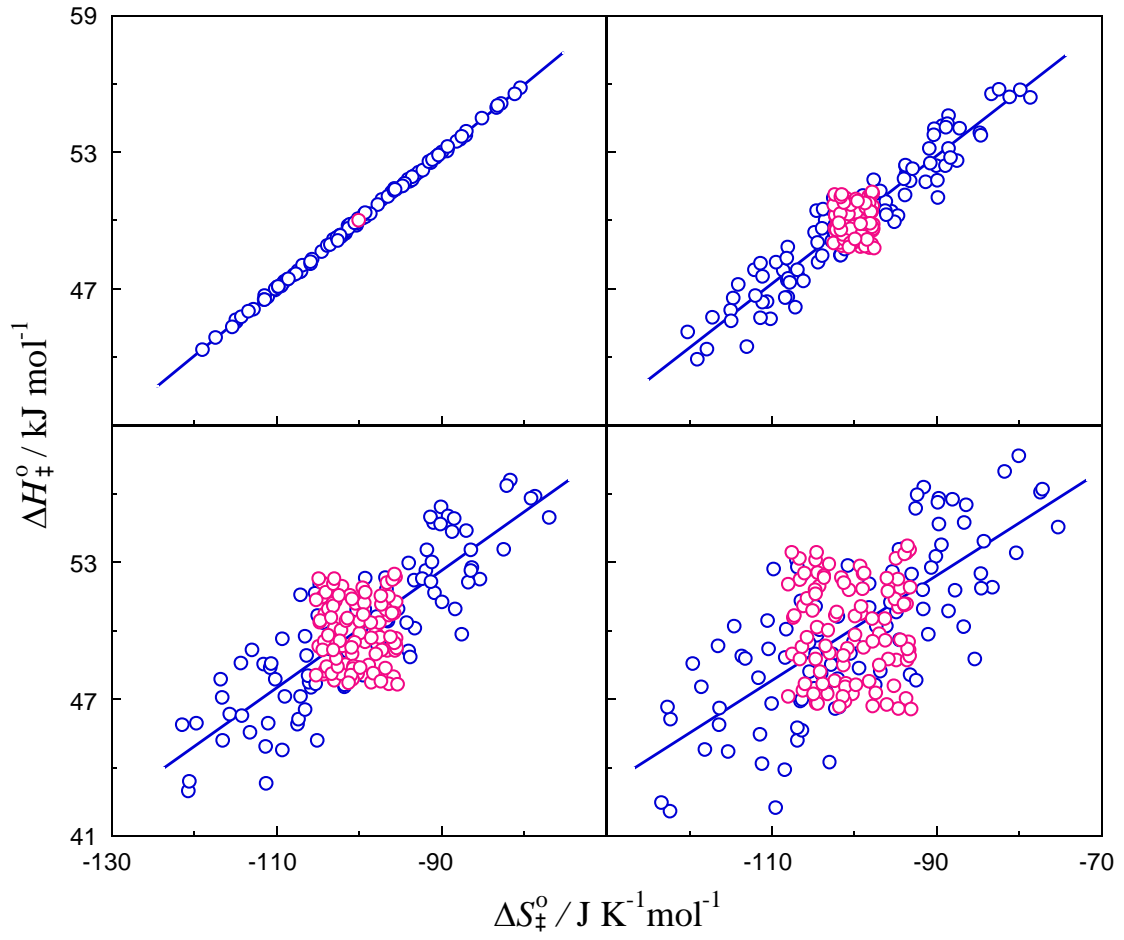


Figure 2. Activation enthalpy as a function of the activation entropy for simulations performed with $T_m = 298.15$ K, $\Delta T = 20.0$ K, $\Delta H_{\neq,m}^0 = 50$ kJ mol⁻¹, $\Delta S_{\neq,m}^0 = -100$ J K⁻¹ mol⁻¹, $F = 0.00$ (left top), 0.25 (right top), 0.50 (left bottom) and 0.75 (right bottom), and $N = 100$. Purple points: in the absence of experimental errors ($Q = 0$). Blue points: in the presence of experimental errors ($Q = 1$).

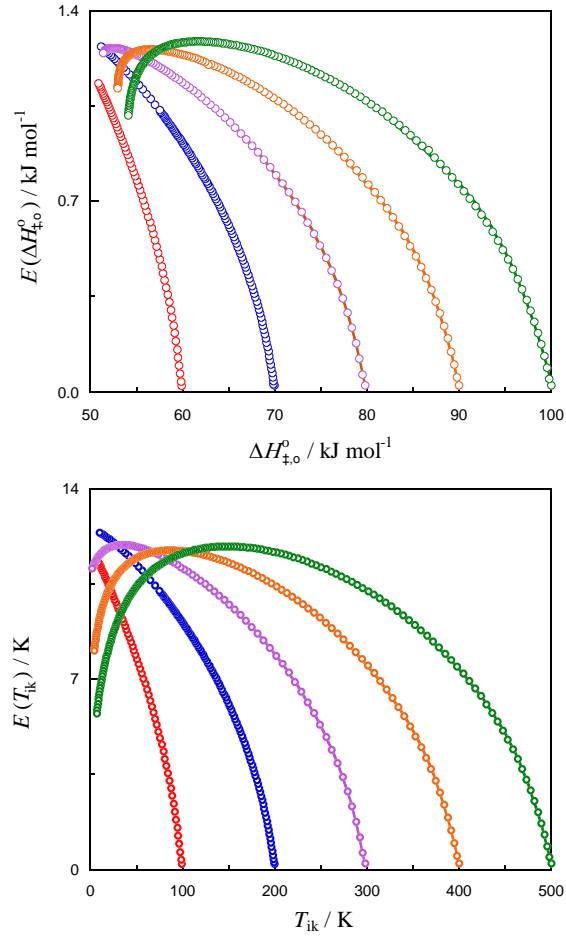


Figure 3. Intercept absolute error as a function of the intercept value (top) and slope absolute error as a function of the slope value (bottom) corresponding to the enthalpy-entropy compensation straight lines for simulations performed with $T_m = 100$ (red), 200 (blue), 298.15 (violet), 400 (orange) and 500 (green) K, $\Delta T = 20.0$ K, $\Delta H_{\ddagger,m}^0 = 50 \text{ kJ mol}^{-1}$, $\Delta S_{\ddagger,m}^0 = -100 \text{ J K}^{-1} \text{ mol}^{-1}$, $F = 0.00 - 8.65$, $Q = 1$ and $N = 1000$.

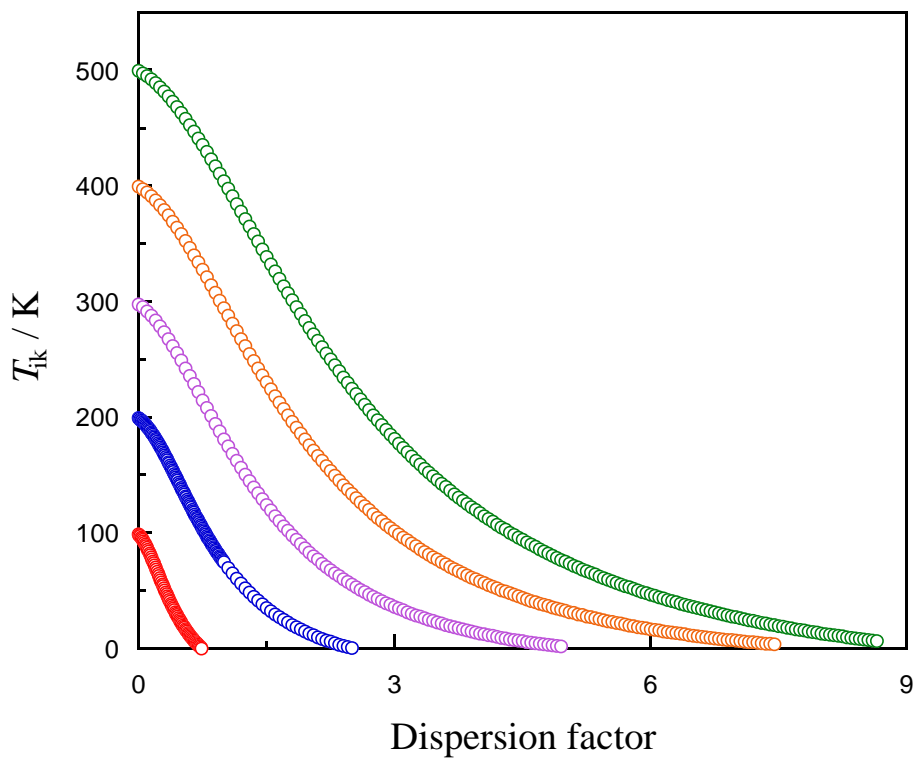


Figure 4. Apparent isokinetic temperature as a function of the dispersion factor corresponding to the enthalpy-entropy compensation straight lines for simulations performed with $T_m = 100$ (red), 200 (blue), 298.15 (violet), 400 (orange) and 500 (green) K, $\Delta T = 20.0$ K, $\Delta H_{\neq, m}^o = 50 \text{ kJ mol}^{-1}$, $\Delta S_{\neq, m}^o = -100 \text{ J K}^{-1} \text{ mol}^{-1}$, $F = 0.00 - 8.65$, $Q = 1$ and $N = 1000$.

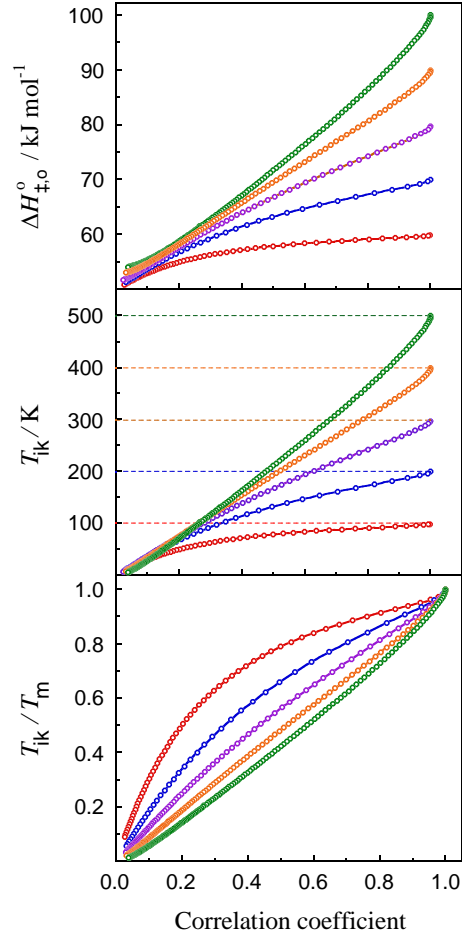


Figure 5. Intercept (top), slope (middle) and ratio between the apparent isokinetic temperature and the mean experimental temperature (bottom) as a function of the correlation coefficient corresponding to the enthalpy-entropy compensation straight lines for simulations performed with $T_m = 100$ (red), 200 (blue), 298.15 (violet), 400 (orange) and 500 (green) K, $\Delta T = 20.0$ K, $\Delta H_{\neq,m}^o = 50$ kJ mol⁻¹, $\Delta S_{\neq,m}^o = -100$ J K⁻¹ mol⁻¹, $F = 0.00 - 8.65$, $Q = 1$ and $N = 1000$.

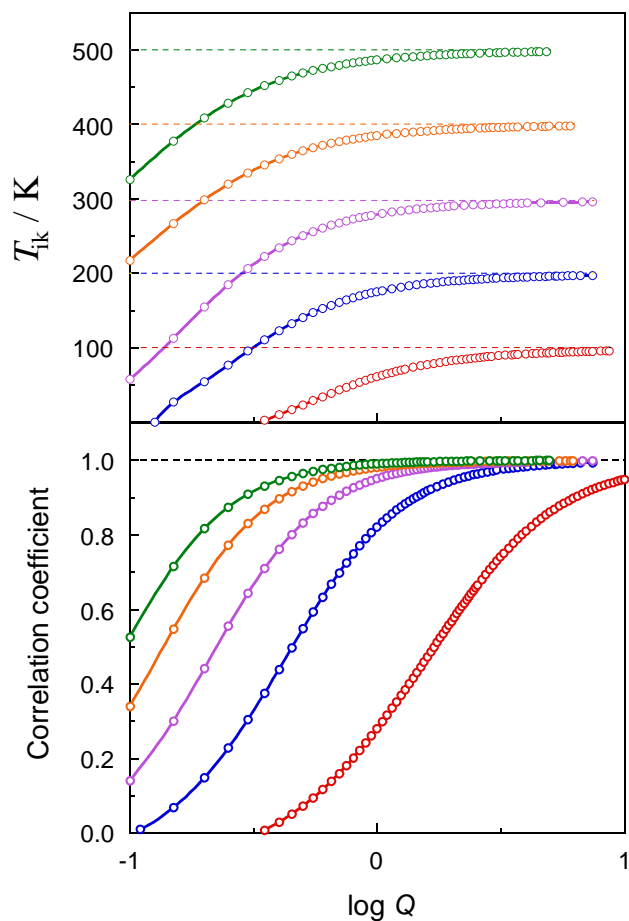


Figure 6. Apparent isokinetic temperature (top) and correlation coefficient (bottom) as a function of the logarithm of the experimental error coefficient of the rate constants corresponding to the enthalpy-entropy compensation straight lines for simulations performed with $T_m = 100$ (red), 200 (blue), 298.15 (violet), 400 (orange) and 500 (green) K, $\Delta T = 20.0$ K, $\Delta H_{\neq, m}^o = 50 \text{ kJ mol}^{-1}$, $\Delta S_{\neq, m}^o = -100 \text{ J K}^{-1} \text{ mol}^{-1}$, $F = 0.25$, $Q = 0.1 - 8.7$ and $N = 1000$.

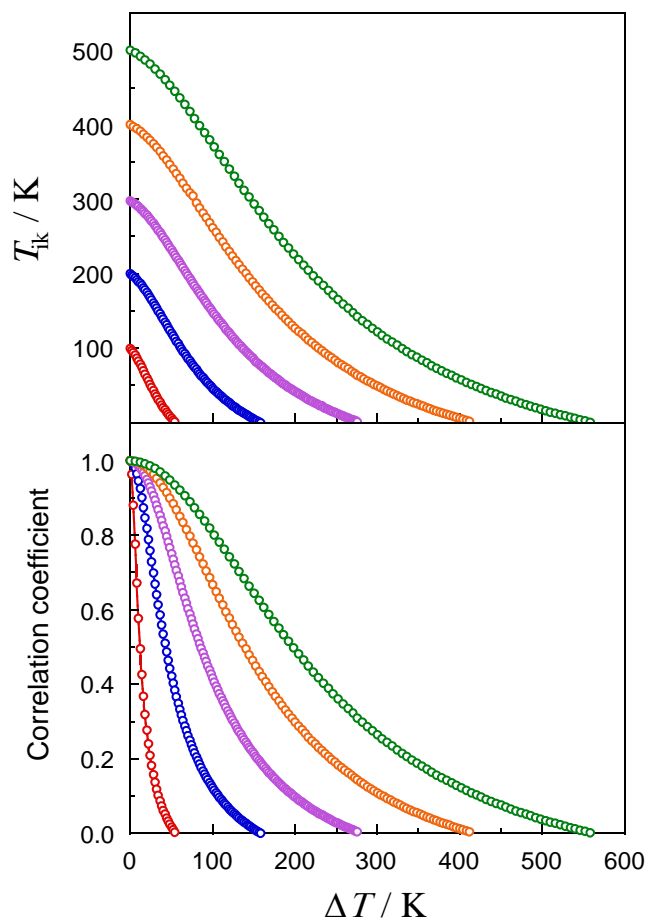


Figure 7. Apparent isokinetic temperature (top) and correlation coefficient (bottom) as a function of the difference between the maximum and minimum values of the experimental temperature corresponding to the enthalpy-entropy compensation straight lines for simulations performed with $T_m = 100$ (red), 200 (blue), 298.15 (violet), 400 (orange) and 500 (green) K, $\Delta T = 0.2 - 558.2$ K, $\Delta H_{\neq, m}^o = 50 \text{ kJ mol}^{-1}$, $\Delta S_{\neq, m}^o = -100 \text{ J K}^{-1} \text{ mol}^{-1}$, $F = 0.25$, $Q = 1$ and $N = 1000$.

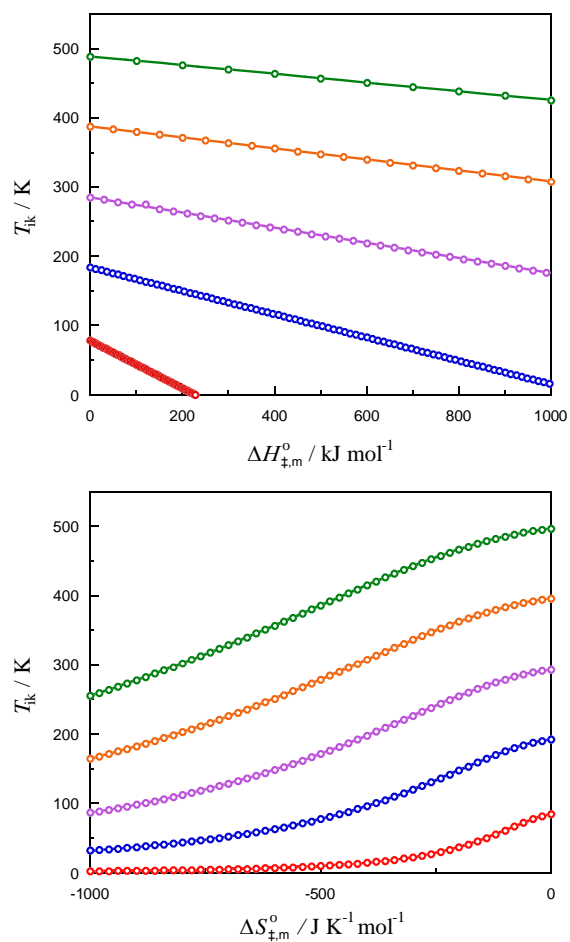


Figure 8. Apparent isokinetic temperature as a function of either the mean activation enthalpy (top, $\Delta S_{\ddagger,m}^0 = -100 \text{ J K}^{-1} \text{mol}^{-1}$) or the mean activation entropy (bottom, $\Delta H_{\ddagger,m}^0 = 50 \text{ kJ mol}^{-1}$) corresponding to the enthalpy-entropy compensation straight lines for simulations performed with $T_m = 100$ (red), 200 (blue), 298.15 (violet), 400 (orange) and 500 (green) K, $\Delta T = 20.0 \text{ K}$, $F = 0.25$, $Q = 1$ and $N = 1000$.

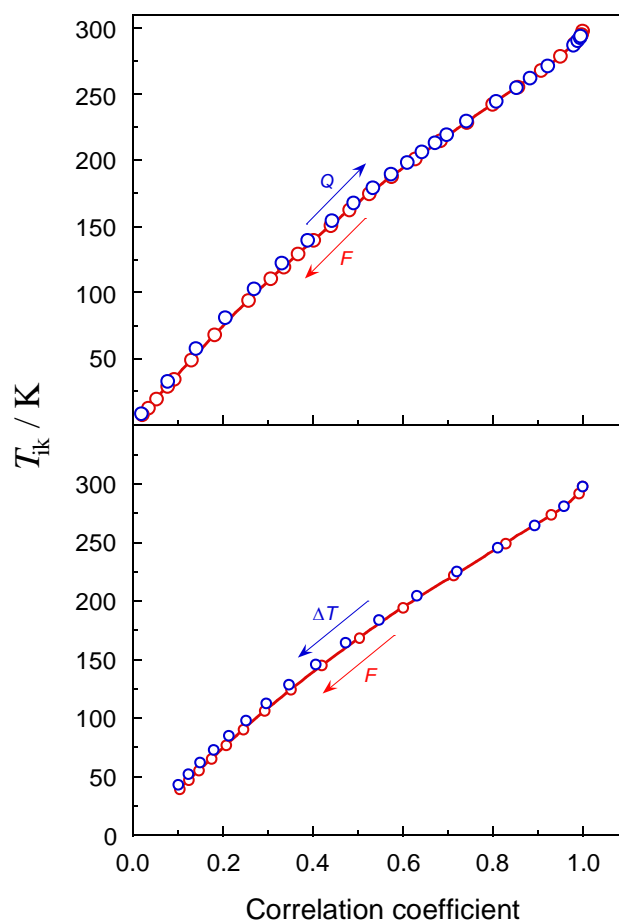


Figure 9. Apparent isokinetic temperature as a function of the correlation coefficient corresponding to the enthalpy-entropy compensation straight lines for simulations performed with $T_m = 298.15$ K, $\Delta H_{\neq, m}^o = 50$ kJ mol⁻¹, $\Delta S_{\neq, m}^o = -100$ J K⁻¹ mol⁻¹ and $N = 1000$. Top: $\Delta T = 20.0$ K; red: $F = 0.0 - 4.4$, $Q = 1$; blue: $F = 0.25$, $Q = 0.06 - 4.00$. Bottom: $Q = 1$; red: $\Delta T = 20.0$ K, $F = 0.0 - 4.4$, blue: $\Delta T = 0.2 - 198.2$ K, $F = 0.25$. The arrows indicate the direction in which the variable parameter increases.

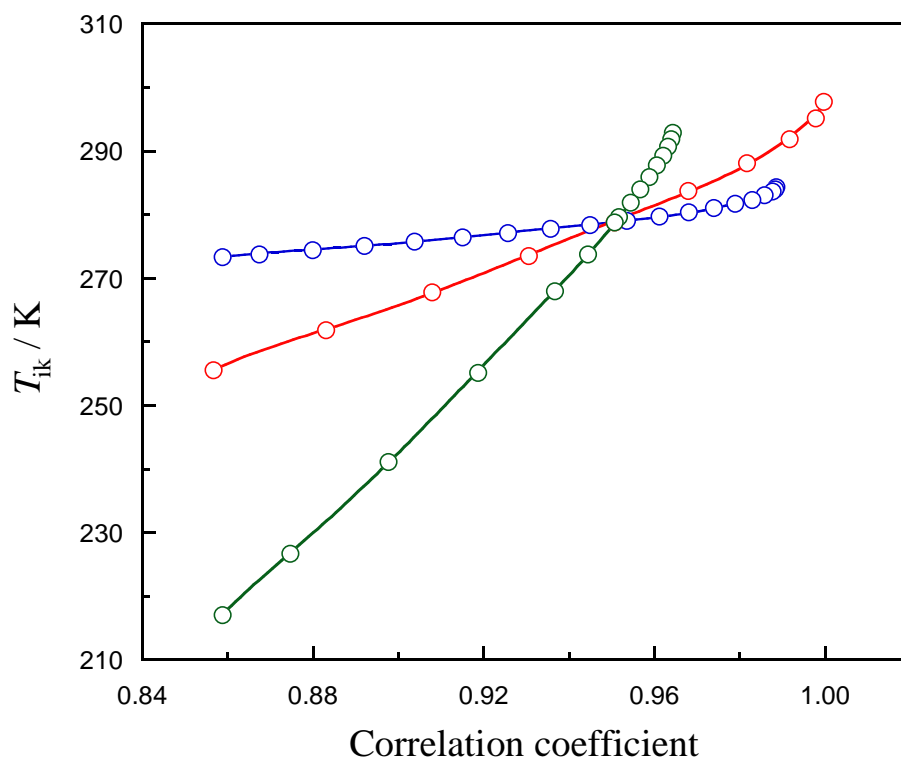


Figure 10. Apparent isokinetic temperature as a function of the correlation coefficient corresponding to the enthalpy-entropy compensation straight lines for simulations performed with $T_m = 298.15$ K, $\Delta T = 20.0$ K, $Q = 1$ and $N = 1000$. Red: $\Delta H_{\neq, m}^o = 50$ kJ mol⁻¹, $\Delta S_{\neq, m}^o = -100$ J K⁻¹ mol⁻¹, $F = 0.00-4.95$. Blue: $\Delta H_{\neq, m}^o = 0-100$ kJ mol⁻¹, $\Delta S_{\neq, m}^o = -100$ J K⁻¹ mol⁻¹, $F = 0.25$. Green: $\Delta H_{\neq, m}^o = 50$ kJ mol⁻¹, $-\Delta S_{\neq, m}^o = 0-332$ J K⁻¹ mol⁻¹, $F = 0.25$.

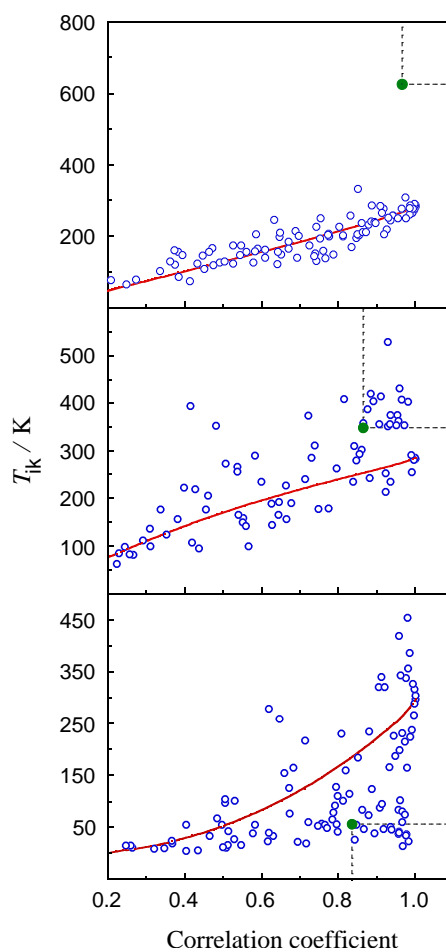


Figure 11. Isokinetic temperature as a function of the correlation coefficient for the application of the p -test to three homologous reaction series. Red lines: maximum probability curves. Blue points: simulation data. Green points: experimental data from ref. 1 (top), 25 (middle) and 26 (bottom). The dashed lines show the limits of the quadrants corresponding to potentially valid simulations.

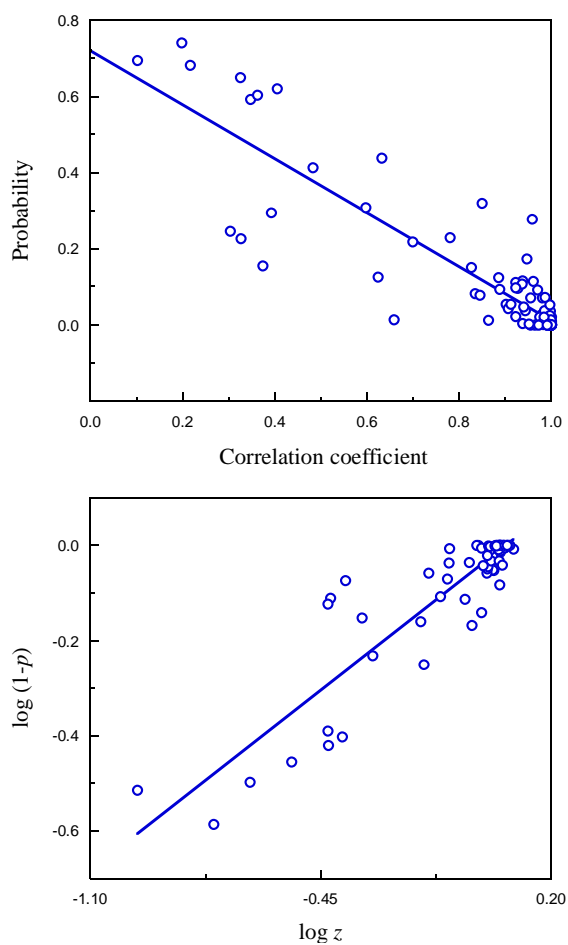


Figure 12. Probability parameter as a function of the correlation coefficient (top) and its dependence on the statistically-weighted combination of N_{exp} , F_{max} , $T_{\text{ik}}/T_{\text{m}}$ and r (bottom) for the results obtained by application of the p -test to 100 homologous reaction series taken from bibliographic sources.

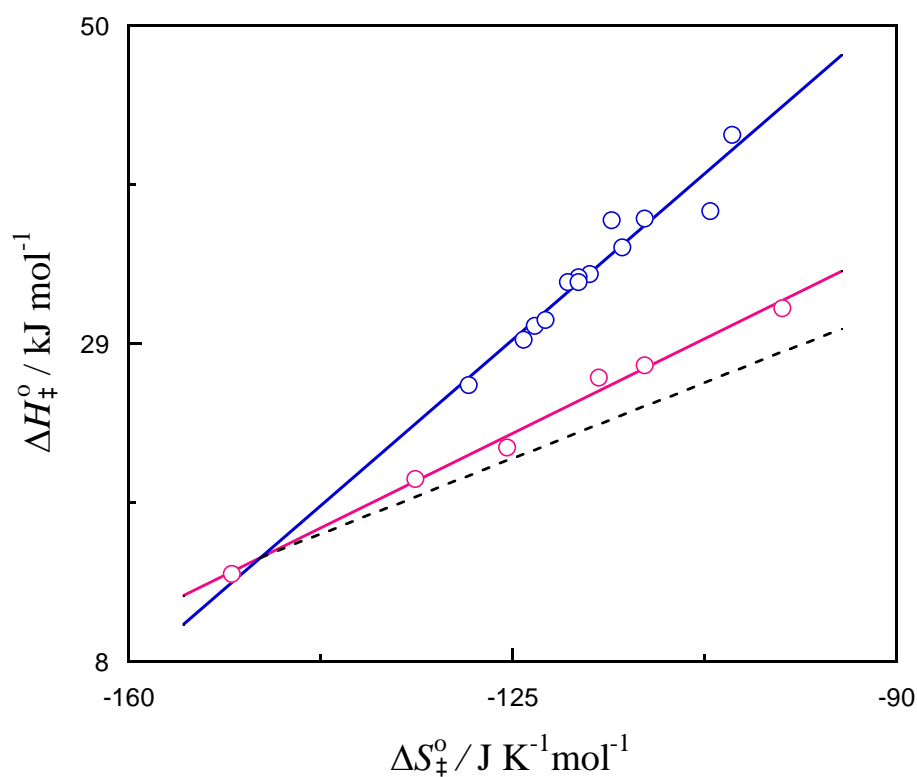


Figure 13. Experimental isokinetic plots for the permanganate oxidation of two homologous series of alkenes containing a functionalized terminal group. Purple points: oxidant: permanganate ion; reductants (from left to right): cinnamate ion, crotonate ion, acrylate ion, 3-butenate ion, 4-pentenoate ion and allyl alcohol; solvent: water (ref. 41). Blue points: oxidant: tributylmethylammonium permanganate; reductants: cinnamic acid derivatives containing the substituents (from left to right) *m*-NO₂, *m*-CF₃, *m*-Cl, *m*-Br, 3-D, *m*-OCH₃, 2-D, none, 2-CH₃, *p*-CH₃, *o*-OCH₃, *p*-OCH₃ and 2-C₆H₅; solvent: dichloromethane (ref. 1). The dashed line corresponds to a linear correlation with slope = $T_m = 286$ K.

“Table of Contents” Graphic

